Research Article | Vol. 59, No. 34 / 1 December 2020 / Applied Optics 10719

applied optics

# Stray light nonuniform background correction for a wide-field surveillance system

**Zeming Xu,[1,2] Dan Liu,[1,2] Changxiang Yan,[1,3,*] and Chunhui Hu[1]**

[1]Changchun Institute of Optics, Fine Mechanics and Physics, Chinese Academy of Sciences, Changchun 130033, China
[2]University of Chinese Academy of Sciences, Beijing 100049, China
[3]College of Materials Science and Opto-Electronic Technology, University of Chinese Academy of Science, Beijing 100049, China
*Corresponding author: yancxciomp@163.com

Received 7 August 2020; revised 30 October 2020; accepted 2 November 2020; posted 3 November 2020 (Doc. ID 404685); published 30 November 2020

**Wide field and a long exposure time can effectively improve the ability of a space surveillance telescope to detect faint space targets. However, such systems are very susceptible to stray light. A stray light nonuniform background will cause great interference to subsequent target recognition, resulting in a large number of false alarms. This study presents an accurate and robust correction algorithm, called the improved new top-hat transformation (INTHT), for a stray light nonuniform background. First, we analyzed the formation mechanism and influence of the stray light nonuniform background. Then, to retrieve the lost targets, the size relationship of the two different, but related, structural operators is changed so the sizes of two structural operators are not equal. Finally, before comparing to the original image to take the minimum value, we added an expansion operation to restore the background size transformation caused by the different sizes of the structural operators in the previous step. This will ensure that there is no residual stray light nonuniform background. We believe, to the best of our knowledge, that the experimental results for the real captured image datasets demonstrate that, compared to other algorithms, the proposed INTHT algorithm has a higher accuracy and effectiveness in correcting a stray light nonuniform background.** 

https://doi.org/10.1364/AO.404685

## 1. INTRODUCTION

With the development of human space activities, the number of space targets (including nonfunctional artificial objects, apogee boost, and spent upper stages) has rapidly increased [1,2]. If such a large number of space targets collide with one other, then this will become a remarkable threat to human space activities [3]. To meet the requirement for the safety of the space environment and the increasing demand for the detection of faint targets in deep space, using a space surveillance telescope detection optical system with a wide field of view (FOV) and a long exposure time has become a major trend, as emphasized by China's Fengyun satellite program [4] and the U.S. Space-Based Space Surveillance (SBSS) project [5,6]. However, despite such optical sensors, the problem of stray light is always an important research issue [7,8]. Since the surveillance image is the only data source for the space surveillance telescope system, the presence of stray light is fatal for its performance. Stray light will bring a very serious nonuniform background signal to the surveillance image and confuse the energy distribution; then, the dynamic range and clarity of the image will be reduced [9]. In particular, the existence of a stray light nonuniform background will seriously affect the effective segmentation of targets and the background when performing subsequent target recognition and extraction, which will lead to a large number of false alarms. Therefore, research on the correction method for the stray light nonuniform background for the surveillance image is urgent. An effective distinction target and background is a necessary prerequisite for target recognition and extraction.

In recent years, the stray light problem has increasingly become an important factor limiting the performance of the instrument, especially in the field of dim and small target tracking and measurement [10–13]. Many stray light nonuniform background correction methods have been proposed, and these can be roughly divided into two types: calibration based and scene based. The calibration-based correction methods are relatively simple and convenient, since they obtain calibration parameters based on previously collected uniform images. The nonuniform background resulting from stray light can be overcome to some extent by such methods [14–16]. However, since the surveillance image contains a large number of stars, space targets, and complex and a varied stray light nonuniform background, we cannot obtain relatively accurate correction parameters. In addition, because the target position and stray light background between different frames are different, a single correction data will cause a large number of targets to not be detected or cause a large number of false alarms. The scene-based correction methods can estimate stray light nonuniform background according to the difference information between the target and the background in an image without calibration reference. Since only the image itself is considered, such methods can be adapted to any scene. For scene-based nonuniform background correction methods, there are mainly two options: wavelet-based algorithms and curvelet-based algorithms [17–19]. These frequency-domain-based methods cannot correct the nonuniform background caused by stray light in a surveillance image. On the one hand, these algorithms are too complicated, and we cannot spend a lot of processing time in the preprocessing stage. On the other hand, a surveillance image with a low signal-to-noise ratio (SNR) will affect the performance of these algorithms, resulting in a large number of target losses or false alarms [20]. To solve the problem, some filter-based algorithms based on a spatial domain have been proposed, such as maximum median filtering, maximum mean filtering [21], a one-dimensional/two-dimensional (1D/2D) morphology operation [22–24], and mean iterative filtering [25]. The above methods have good nonuniform correction capabilities in different fields, but these algorithms are very sensitive to the size of the structural operator, so an inappropriate structural operator size will seriously affect the performance of these filter-based algorithms. As a result, how to accurately and quickly correct the nonuniform background caused by stray light in the surveillance image is still an urgent problem not yet solved.

To overcome the defects of existing methods, we propose a stray light nonuniform background correction method called improved new top-hat transformation (INTHT). Specifically, the INTHT method has three main stages. In the first stage, we analyzed in detail the formation mechanism and influence of a stray light nonuniform background. Although we cannot get accurate parameters to use the calibration-based correction method, analyzing the cause of problem offers important guidance on how to improve the accuracy and robustness of the algorithm. In the second stage, inspired by this new top-hat transformation, Jiang *et al.* used the new top-hat transformation to improve the accuracy of the star segmentation. Due to the different sizes of targets in the surveillance image, the method will cause some targets to be lost. We applied the new relationships between the structural operators to the surveillance image; that is, we made significant changes to the new top-hat transformation and redefined it.

In the third stage, we first break the limitation of the size relationship between the two structural operators in the new top-hat transformation to retrieve the lost target. Then, before comparing to the original image to take the minimum value, we add an expansion operation step to restore the background size transformation caused by the different sizes of the structural operators in the previous step, to ensure that there is no residual stray light nonuniform background. This also greatly reduces the sensitivity of the algorithm to structural operators. Further experimental results for real captured image datasets demonstrate that the proposed INTHT algorithm has higher accuracy and robustness in correcting a stray light nonuniform background.

## 2. FORMATION MECHANISM AND INFLUENCE OF STRAY LIGHT

Stray light in an imaging system is the ray that does not come from the target, but reaches the sensors or the one that comes from the target ending on the sensor via abnormal means. In this section, we will analyze in detail the formation mechanism and influence of the nonuniform background caused by stray light in the surveillance image. In our previous work [26], we have analyzed in detail the effects of stray light from nontarget light sources and proposed a new vane structure optimization method to suppress the influence of strong stray light sources. Although the intensity of stray light has dropped to an acceptable level, the weakened stray light will still affect the surveillance image. Specifically, a strong stray light, after being weakened entering the optical system, will add a nonuniform background to the focal plane detector. It increases the gray for the entire surveillance image, and its grayscale diffuses from one edge of the surveillance image to the other. The result of 3D ray tracing in LightTools is shown in Fig. 1(a). The main reason for this

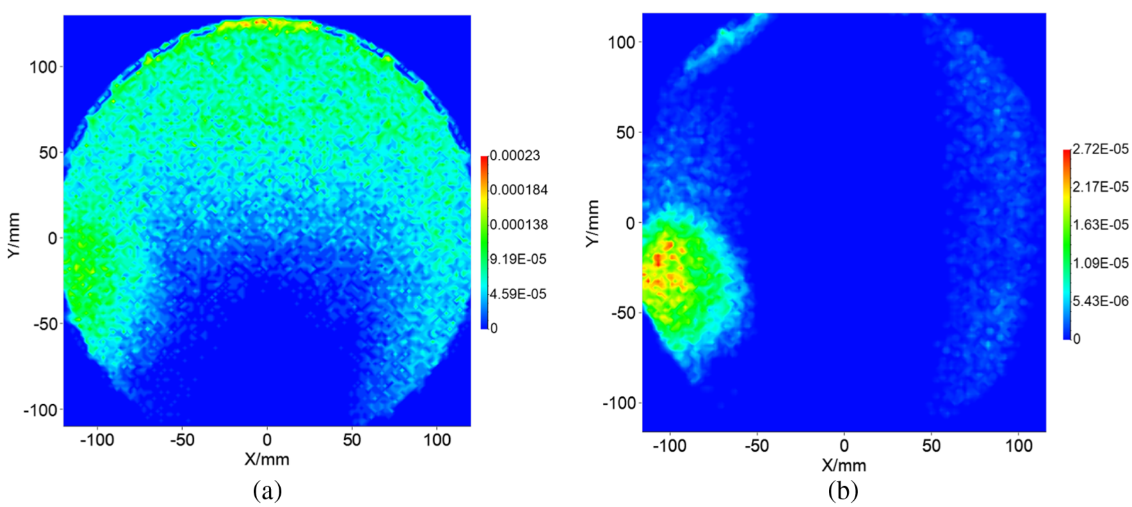


**Fig. 1.** (a) 3D ray tracing diagram of Type I stray light background. (b) 3D ray tracing diagram of type II stray light background.

situation is that the scattering intensity of the material surface is gradually changing. In addition, because it is stray light from outside the field of view, the grayscale value is the maximum at the corresponding edge of the image. We called this type of stray light background Type I stray light background.

For stray light formed by the target light sources, it will also add a nonuniform background to the focal plane detector. However, its formation mechanism and impact on the surveillance image are completely different from Type I stray light background. Although it also increases the gray value of the surveillance image different from Type I, this causes a relatively bright region to appear in the surveillance image and its gray value spreads from its center to the surrounding. The result of 3D ray tracing in LightTools is shown in Fig. 1(b). We named this type of stray light background as Type II stray light background. The formation mechanism of the Type II stray light background is due to the total reflection phenomenon in the lens when the presence of brighter star in the field of view and incident at a specific angle.

Type I and Type II are the fundamental reasons for the existence of the stray light nonuniform background. In addition, any complex stray light background can be understood as a combination of these two types of stray light. Therefore, we call this mixed stray light Type III. For mixed stray light, it will also add a nonuniform stray light background to the focal plane detector. The effect of Type III stray light on the grayscale of the surveillance image depends on the combination of Type I and Type II stray light. Strictly speaking, we will optimize the design of the baffle and choose appropriate working hours to avoid stray light as much as possible, and. Type III stray light may not happen in the system of this paper. However, for the completeness of the analysis, we briefly outline this situation.

## 3. STRAY LIGHT CORRECTION METHOD

In this section, we will introduce in detail how to correct the nonuniform background caused by stray light, to ensure the effective recognition of subsequent space targets and stars.

### A. Analysis of the Principle of Stray Light Nonuniform Background Correction

The surveillance image is modeled as

$$F(i, j, k) = T(i, j, k) + S(i, j, k) + B(i, j, k) + N(i, j, k), \quad (1)$$

where $k$ is the frame index of the surveillance image sequence, and $F(i, j, k)$ represents the grayscale value at the integer space coordinate $(i, j)$ in the $k-$th frame of the surveillance image sequence. $T(i, j, k)$ and $S(i, j, k)$ denote the space targets and stars, respectively. $B(i, j, k)$ refers to the nonuniform background caused by stray light. Its formation mechanism and impact on the surveillance image are as analyzed above. $N(i, j, k)$ is the noise of the surveillance image.

The basic idea of stray light correction is how to accurately and quickly estimate $B(i, j, k)$ while retaining $T(i, j, k)$ and $S(i, j, k)$. Since we know that we cannot use the calibration-based correction method in the surveillance image, we can only use the scene-based correction method. For scene-based correction methods, accurate use of the difference information between the target region and the background region is the key to the method, which also determines the performance of various scene-based methods.

For some frequency-domain-based correction methods that have achieved good results in other fields, it is difficult to correct the stray light nonuniform background in the surveillance images. Because the surveillance image contains a large number of stars and space targets, with greatly different sizes and intensity differ, it is difficult for us to accurately distinguish stars, space targets, and the stray light background when transformed to the frequency domain. Because filter-based methods based on the spatial domain use the structural operator (that is, only the pixel values of the target region and its surrounding region are considered), the effect of these methods is significantly better than methods based on the frequency domain. In addition, although the background of the image is nonuniform, the gray value of the target is always higher than the surrounding background gray value of the target region. However, these filter-based methods still have certain problems when processing surveillance images. On the one hand, because all the pixels in the structural operator including the target region and its surrounding region are involved in the calculation, this will seriously affect the accuracy of the estimation of the stray light nonuniform background. On the other hand, filter-based methods are very sensitive to the selection of the size of the structural operator, which will cause the loss of targets when correcting the stray light nonuniform background. How to choose structural operators to satisfy different surveillance images is still unresolved.

### B. Improved New Top-Hat Transformation Correction Algorithm

To improve the accuracy of stray light correction based on the filtering method and reduce the sensitivity of the filtering method to the operator size, we propose an improved new top-hat transformation (INTHT) correction algorithm. The operation and principle of the proposed INTHT correction algorithm are explained below.

In the INTHT method, the two structural operators $\Delta B = B_o - B_i$ and $B_b$ of the proposed INTHT correction algorithm are shown in Fig. 2(a) and Fig. 2(b), respectively. Where $B_i$ and $B_o$ are, respectively, defined as the inner structural operator and the outer structural operator of the structural operator $\Delta B$, $K$, $L$, and $M$ represent the size of $B_i$, $B_o$, and $B_b$, respectively, $M > L > K$. Because we use the structural operator $\Delta B = B_o - B_i$, this makes the pixel value of the target region involved in the calculation of the filtering operation very few or zero. The principle is as follows.

First, we use the structural operator $\Delta B = B_o - B_i$ to perform a dilation operation on the surveillance image to obtain the image $F_1$, so

$$F_1 = F \oplus \Delta B = \max\{F(i-m, j-n) + \Delta B(m, n) | (i-m), (j-n) \in D_F, (m, n) \in D_{\Delta B}\}, \quad (2)$$

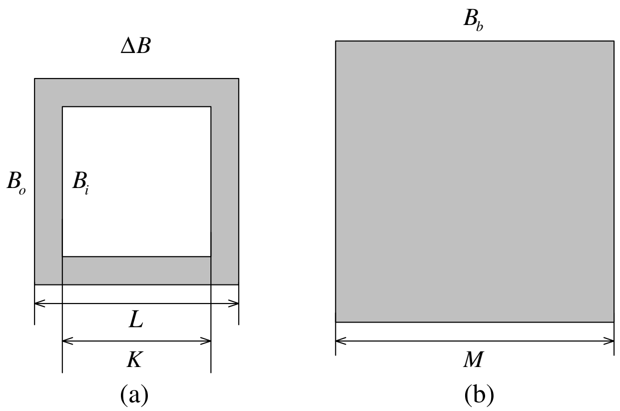


**Fig. 2.** Used structural operators in the proposed INTHT correction algorithm.

where $D_F$ and $D_{\Delta B}$ represent the domain of $F$ and $\Delta B$, respectively. According to the definition of the structural operator $\Delta B$, only the surrounding background pixels of target region are involved in the calculation of the dilation operation of Eq. (2). Because of the definition domain of $\Delta B$, targets with a size smaller than $K$ will not participate in the dilation operation at all; that is, to replace the pixels of the target region with the pixels in the surrounding region. As shown in Fig. 3(b), the purpose of structural operator $\Delta B$ is to better protect the target region and reduce the number of target region pixels involved in the stray light background estimation. This will fundamentally improve the accuracy of the stray light nonuniform background correction.

Then we use a structural operator $B_b$ with a size greater than $L$ to perform an erosion operation on the image $F_1$, so

$$F_2 = F_1 \Theta B_b = \min\{F_1(i+m, j+n) - B_b(m,n) | (i+m), (j+n) \in D_{F_1}, (m,n) \in D_{B_b}\}, \tag{3}$$

where $D_{F_1}$ and $D_{B_b}$ represent the domain of $F_1$ and $B_b$, respectively. Since there are a large number of stars and space targets in the surveillance image and their sizes are completely different, the fixed structural operator cannot apply to all targets. Although most of the targets will be well retained after the dilation operation of Eq. (2), some pixels of a few larger-sized targets will still be mistaken for the stray light background and remain in the image $F_1$. Therefore, using the structural operator $B_b$ to perform the erosion operation on the image $F_1$ can retrieve all the lost targets because the size of the structural operator $B_b$ can be relatively large. The result of this process is shown in Fig. 3(c).

At this time, the image $F_2$ will only be the stray light background that must be deleted. However, because the size of structural operator of the erosion operation is larger than that of the dilation operation (that is, $B_b > \Delta B$), this makes the stray light background region that must be corrected smaller. In other words, there will be just residual stray light background. Therefore, we use the structural operator $B_b$ to perform a dilation operation on image $F_2$, as shown in Eq. (4). This will ensure that the stray light nonuniform region that must be corrected will not change. The result of this process is shown in Fig. 3(d), so

$$F_3 = F_2 \oplus B_b = \max\{F_2(i-m, j-n) + B_b(m,n) \left| (i-m), (j-n) \in D_{F_2}, (m,n) \in D_{B_b} \right\}. \tag{4}$$

It should be noted here, because we use the structural operator $\Delta B$ in the dilation operation to replace the pixels of the target region with the pixels in the surrounding regions to protect the target. Therefore, if the processed region is not a target region, the relationship of the pixels in the processed and surrounding regions is not confirmed. To ensure accuracy, the final stray light background that must be deleted is

$$F_4 = \min(F, F_3), \tag{5}$$

where $F_4$ is the final stray light background that must be deleted.

Therefore, the final corrected surveillance image $F_c$ is

$$F_c = F - \min\{F, (F \oplus \Delta B \Theta B_b \oplus B_b)\}. \tag{6}$$

Through the above method, the surveillance image affected by stray light can be accurately corrected.

### C. Selection of Size Parameters of Structural Operators

Through Section 3.B, we can accurately correct the stray light background. However, we need to choose reasonable size parameters of the structural operators; otherwise, unreasonable size parameters will greatly reduce the practicability of the proposed INTHT correction algorithm.

From Eq. (2), we use the structural operator $\Delta B$ to preserve the target and replace the pixels of the target region with the pixels in the surrounding region, so the choice of the structural

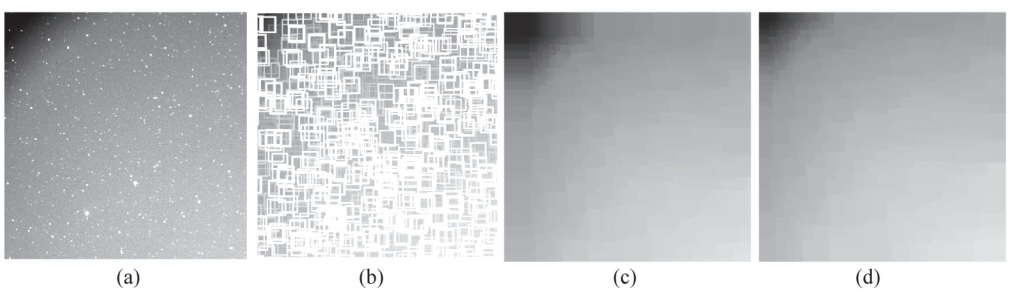


**Fig. 3.** Figures of processing results after Eq. (2), Eq. (3), and Eq. (4), respectively. (a) Original surveillance image. (b) Processing result of Eq. (2). (c) Processing result of Eq. (3). (d) Processing result of Eq. (4).

operator $\Delta B$ is extremely important; that is, the choice of parameters $K$ and $L$ is extremely important.

For parameter $K$, since the vast majority of the stars and space targets in the surveillance images we have collected in the past have a size range of less than $25 \times 25$ pixels, the value of $K$ can be selected from 0 to 25 according to the surveillance image. Proper selection of parameter $K$ can protect stars and space targets as much as possible. In addition, to make the selected parameter $K$ applicable to most surveillance images, reduce the sensitivity of the algorithm to the structural operator, and to protect more targets during the target region replacement process, we choose the value of parameter $K$ to be 25.

For parameter $L$, when the parameter $K$ is determined, the size of parameter $L$ determines the number of pixels in the surrounding background region involved in the calculation in Eq. (2); that is, the larger $L$ is, the more pixels in the surrounding background region will be involved in the calculation of Eq. (2). On the contrary, the smaller $L$ is, the fewer pixels in the surrounding background region will be involved in the calculation of Eq. (2). Since the surveillance image contains a large number of targets, if the parameter $L$ is too large, when performing the operation of Eq. (2), a large number of targets will mistake their neighboring targets as the surrounding background region and use them for background region replacement, thereby interfering with each other. That will not only cause the loss of the target, but also the residual stray light background. Therefore, when the parameter $K$ is determined, we can take the value of the parameter $L$ as $L = K + 2$. On the one hand, it avoids the mutual interference between targets caused by the parameter $L$ being too large. On the other hand, it also ensures that enough of the stray light background region participates in the calculation, thereby ensuring the accuracy of the proposed INTHT correction algorithm.

From Eq. (3) and Eq. (4), the use of structural operator $B_b$ is to correct the stray light background while preserving larger-sized stars and space targets. In the surveillance images, we have collected in the past, the size of all targets will not exceed $45 \times 45$ pixels. In addition, according to the analysis in Section 2, whether it is Type I stray light background or type II stray light background, the size of stray light nonuniform background region is much larger than the target size. Therefore, we choose the value of parameter $M$ to be $60 \times 60$ pixels. On the one hand, it ensures that some unknown targets will not be lost. On the other hand, it can also ensure that some unknown stray light will not be mistakenly regarded as a target and retained because the parameter $M$ is too large.

For the same type of application scenarios, we only need to adjust the parameters appropriately to make the proposed INTHT correction algorithm achieve the expected result.

## 4. EXPERIMENTS AND ANALYSIS

In this section, to validate the advantages of the proposed INTHT correction algorithm, top-hat transformation, mean iterative filtering, and new top-hat transformation are used to perform stray light nonuniform background correction experiments in the same real captured image datasets (600 images). The selection of size parameters for the structural operators of the proposed INTHT correction algorithm is as described in Section 3.C. To ensure fairness, the sizes of the initial structural operators for all algorithms are the same.

### A. Accuracy of Stray Light Correction

For the system in this paper, the data acquisition method is the sidereal tracking mode, where the telescope photographs the same area of the sky. The real surveillance image used in the experiments was captured by the telescope equipped with a CMOS sensor with 2s exposure time, and have $10K \times 10K$ imaging pixels, a $10° \times 10°$ field of view, and 12 bits of grayscale. Some results are shown in Fig. 4. In Fig. 4, (a) and (c) are the surveillance images with a Type I stray light nonuniform background, (b) and (d) are the surveillance images with a Type II stray light nonuniform background, and $(a_n) - (d_n)$ are the surveillance images corrected by different methods.

To analyze the accuracy of different algorithms, we use residual analysis to quantitatively evaluate the accuracy of stray light nonuniform background correction of different algorithms. In the residual image, the larger the mean, the higher the overall gray value of the image background, which means that it contains a Type I stray light background. The larger the standard deviation, the higher the degree of fluctuation of the image background distribution, which means that it contains more local region Type II stray light background. Therefore, the mean and standard deviation in the residual image can well reflect the stray light nonuniform background in the image. If the residual mean and residual standard deviation in the surveillance image after correction are smaller, it means that the accuracy of correction algorithm is higher, and there is no residual slowly changing stray light nonuniform background in the corrected surveillance image. In the process of statistical background residual characteristics, it is necessary to avoid the influence of pixels containing space target signals and star signals on the statistical results. Therefore, we introduce the concept of exclusion domain to exclude the influence of the above signals. We use the improved adaptive threshold segmentation algorithm to accurately obtain the excluded domain $E_d$, so

$$E_d(i, j) = \begin{cases} 1, & F_c(i, j) < T \\ 0, & F_c(i, j) > T \end{cases}, \tag{7}$$

where $F_c(i, j)$ represents the corrected surveillance image, $T$ represents the threshold [25]. Therefore, the background residual image $R$ without stars and space targets is

$$R(i, j) = F_c(i, j) E_d(i, j). \tag{8}$$

The 600 surveillance images include 300 surveillance images affected by Type I stray light, and 300 surveillance images affected by Type II stray light. To obtain more accurate statistical results to analyze the performance of the algorithm, we classified the Type I and Type II stray light according to the influence of mean and variance. The statistical results of the background residuals (600 images) from the different methods are shown in Table 1.

From the statistical results in Table 1, we can draw the following conclusions. For the mean iterative method (five iterations), this method does not consider the morphology of the surveillance image, it only uses the gray information in the surveillance

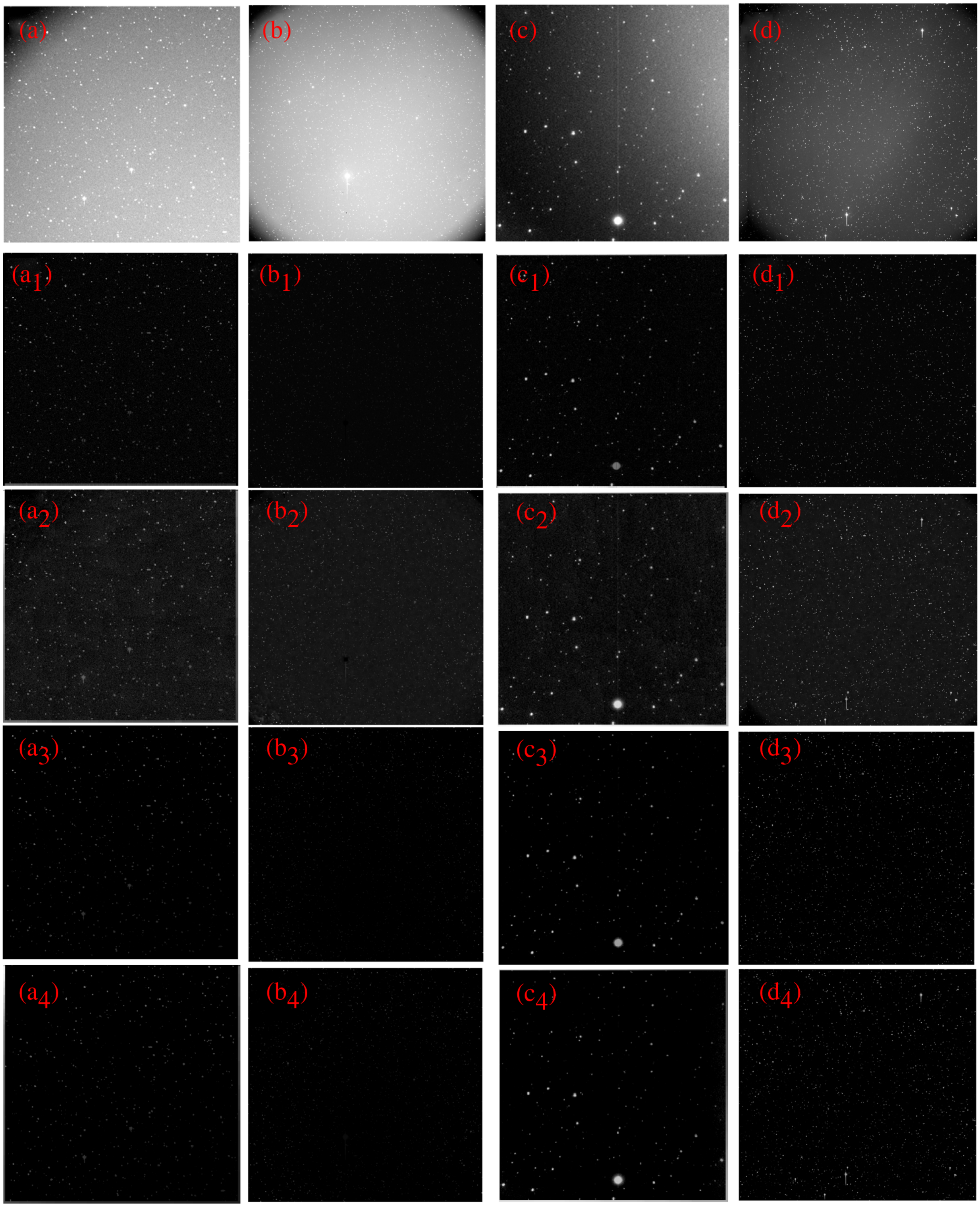


**Fig. 4.** Correction results of four different methods. (a)–(d) Original surveillance images. ($a_1$)–($d_1$) Correction results of mean iterative filtering ($a_2$)–($d_2$) Correction results of top-hat transformation. ($a_3$)–($d_3$) Correction results of new top-hat transformation. ($a_4$)–($d_4$) Correction results of the proposed INTHT method.

image. Therefore, the effect of this method on different types of stray light background correction is almost not much different. For the other three methods based on morphology, the accuracy of stray light background correction depends on the surveillance image type and structural operator. Through the analysis in Section 2 and Section 3.C, we know that as long as the size of structural operator is smaller than the size of the region affected by stray light in the surveillance image, no matter

**Table 1. Statistical Results of the Background Residuals**

| Number of Images | 150 (Type I) | | 150 (Type II) | | 150 (Type I) | | 150 (Type II) | |
|---|---|---|---|---|---|---|---|---|
| Background Residual | Mean | Standard Deviation | Mean | Standard Deviation | Mean | Standard Deviation | Mean | Standard Deviation |
| Original image | 38.2 | 54.1 | 29.6 | 43.1 | 20.0 | 30.0 | 15.9 | 22.8 |
| Mean iterative | 4.8 | 4.2 | 4.4 | 3.8 | 4.2 | 3.7 | 4.1 | 3.6 |
| Top-Hat transformation | 20.8 | 42.9 | 10.9 | 32.1 | 8.9 | 22.1 | 6.2 | 11.7 |
| New Top-Hat transformation | 1.9 | 1.3 | 1.5 | 1.2 | 1.3 | 1.0 | 1.2 | 1.0 |
| Proposed INTHT method | 0.8 | 1.0 | 0.5 | 0.8 | 0.4 | 0.5 | 0.3 | 0.4 |

what type of stray light background, the morphological method can perform stray light background correction. For top-hat transformation, it is better at dealing with a Type II stray light background. Because the Type II stray light background region is smaller, there will be less stray light background involved in the calculation under the same structural operator. Therefore, it is relatively more accurate. However, due to the use of two of the same structural operators in the top-hat transformation, all pixels (including space targets, stars, and background) are involved in the calculation, the effect of stray light nonuniform background correction is poor, and a large amount of stray light nonuniform background will still remain in the corrected surveillance image. For new top-hat transformation and the proposed INTHT method, because the target is replaced first, and then subsequent operations are performed on this basis, they can perform high-precision correction for different types of stray light background. However, because the proposed INTHT method changes the size of structural operators and subsequent operations, more stray light background regions will participate in the subsequent operations, the accuracy of the proposed INTHT method will be greatly improved. In addition, the proposed INTHT method also greatly reduces the sensitivity of the algorithm to the structural operator parameters. The statistical data in Table 1 also shows that the proposed INTHT method can handle surveillance images in a variety of situations.

## B. Target Retention Accuracy Analysis

The stray light nonuniform background correction in the surveillance image is to better improve the accuracy of target recognition. Therefore, algorithms should keep all targets as much as possible while correcting the stray light background. To compare the target retention effects of different algorithms more intuitively, the stray light background eliminated by different algorithms is shown in Fig. 5. In Fig. 5, (a) and (c) are the surveillance images with a Type I stray light nonuniform background, (b) and (d) are the surveillance images with a Type II stray light nonuniform background, and $(a_n) - (d_n)$ are the stray light nonuniform background filtered by different correction methods.

In Fig. 5, it is obvious that the proposed INTHT method has better target retention. To quantitatively analyze the target retention accuracy of different algorithms, the same methods of star and space target recognition are used for the surveillance image corrected by different algorithms. Corresponding to Table 1, the statistical results of the target retention rate are shown in Table 2.

From the statistical results in Table 2, we can draw the following conclusions. For the mean iterative method (five iterations), it only uses the gray information in the surveillance image; therefore, this mean iterative cannot avoid the influence of the highlight region on the background estimation caused by the use of mean, so some brighter stars or space targets in the surveillance image will be mistaken for stray light and filtered out. For top-hat transformation, since the two of the same structural operators are used, all pixels (including space targets, stars, and background) are involved in the calculation and the effect of stray light nonuniform background correction is poor, resulting in a large amount of the stray light background still remaining in the surveillance image. This also brings great interference to the target recognition; in other words, it causes a large number of targets to be lost. For new top-hat transformation, although this algorithm has high accuracy in removing the stray light background, it is too sensitive to the structural operator. A fixed-size structural operator cannot cover all sizes of stars and space targets, resulting in some larger size targets being mistaken for a stray light nonuniform background and lost. For the proposed INTHT method, although the size of the structural operators is also fixed, we reconstruct the size relationship between the structure operators and adjust and add morphological operations. This not only can accurately correct the stray light background to retain more targets, it can also greatly reduces the sensitivity of the algorithm to the structural operator so that the proposed INTHT method can simultaneously correct different types of stray light background. In some cases, the target retention rate cannot reach 100%, mainly because there are too many targets in the surveillance image. This then cause some targets to be too close and interfere with each other (mentioned when the structural operator parameters are determined in Section 3.C). However, the accuracy of the proposed INTHT method is much higher than the existing algorithm. In addition, as long as the size of the structural operator $B_b$ is not greater than the size of the bright spot caused by total reflection (Type II stray light background), the proposed INTHT method can accurately correct the stray light nonuniform background while ensuring that almost all targets are not lost.

## C. Comparison of Computation Time

In Table 3, the computation time for all algorithms applied to a given $10K \times 10K$ test image is shown. These methods are all implemented in MATLAB R2016a, and the PC specifications include an i5-3210M CPU (2.50 GHz) with 8 GB of main memory.

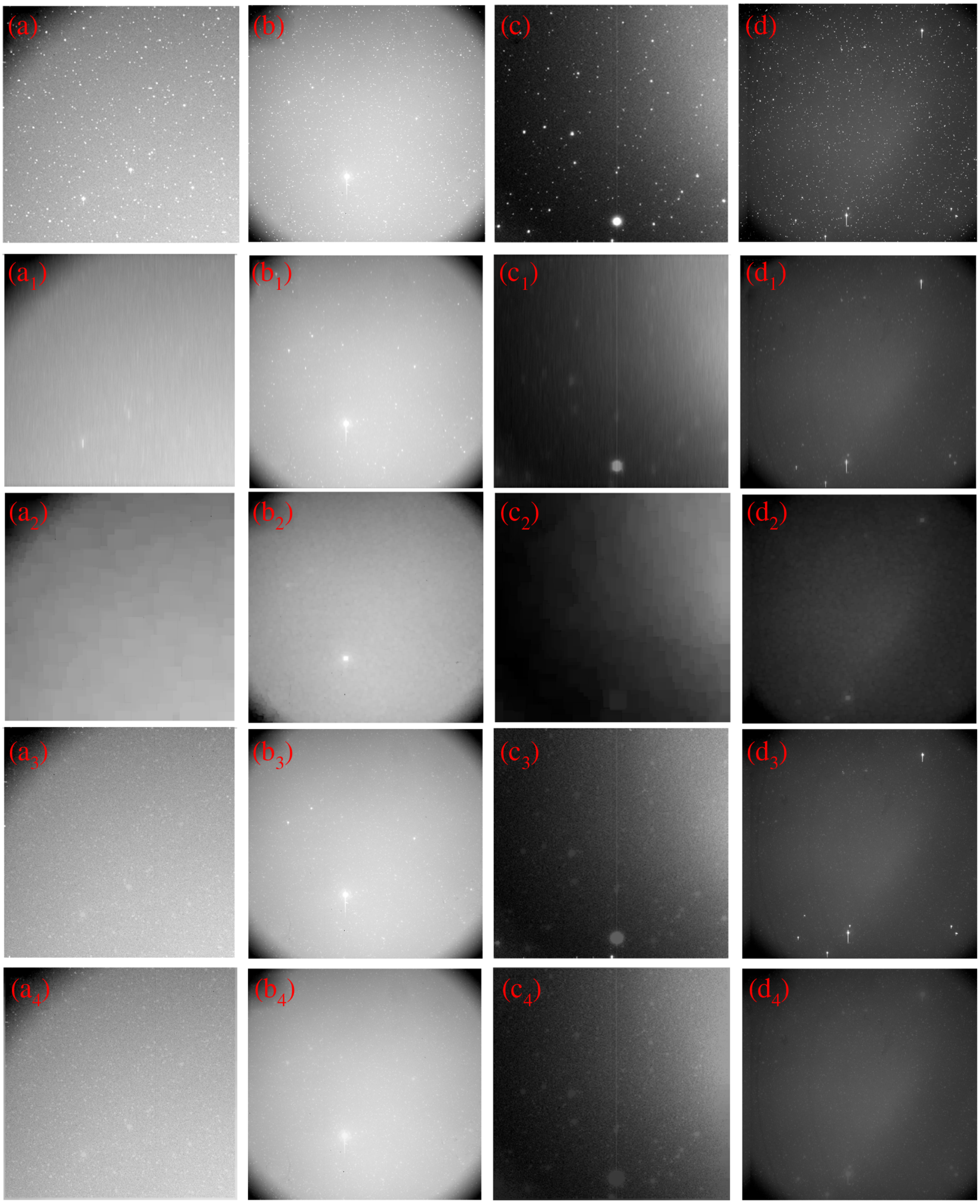


**Fig. 5.** Stray light nonuniform background obtained by four different methods. (a)–(d) Original surveillance images. ($a_1$)–($d_1$) Stray light nonuniform background obtained by mean iterative filtering. ($a_2$)–($d_2$) Stray light nonuniform background obtained by top-hat transformation. ($a_3$)–($d_3$) Stray light nonuniform background obtained by new top-hat transformation. ($a_4$)–($d_4$) Stray light nonuniform background obtained by the proposed INTHT method.

**Table 2. Statistical Results of the Target Retention Rate**

| Number of Images | 150 (Type I) | 150 (Type II) | 150 (Type I) | 150 (Type II) |
|---|---|---|---|---|
| Mean iterative | 90% | 90% | 88% | 89% |
| Top-Hat transformation | 80% | 80% | 85% | 87% |
| New Top-Hat transformation | 90% | 91% | 90% | 92% |
| Proposed INTHT method | 98% | 98% | 99% | 99% |

**Table 3. Statistical Results of Computation Time**

| | Computation Time (s) |
|---|---|
| Mean iterative | 20.13 |
| Top-Hat transformation | 0.52 |
| New Top-Hat transformation | 0.40 |
| Proposed INTHT method | 0.42 |

From the statistical results in Table 3, we can draw the following conclusions. Due to the iterative process, the mean iterative will bring a huge time overhead, which is not allowed for this system. The computation time of the other three algorithms can meet the requirements of the system, but we believe, to the best of our knowledge, that the proposed INTHT method has a higher accuracy and target retention rate.

## 5. CONCLUSION

Since the surveillance image affected by stray light will produce a very serious nonuniform background, the presence of stray light will cause great interference to target recognition and tracking, resulting in a large number of false alarms. How to accurately correct the stray light nonuniform background is a necessary prerequisite for target recognition and tracking.

In this study, we proposed an accurate and robust correction algorithm called INTHT to correct the stray light nonuniform background. First, we analyzed the formation mechanism and influence of the stray light nonuniform background. Analyzing the cause of problem offers important guidance on how to improve the accuracy and robustness of an algorithm. Then, to make full use of the difference information between the target and the surrounding background region, we constructed two different, but related, structural operators. The pixels of the target region are replaced with the pixel value of the surrounding region through the dilation operation so that only the background pixel participates in the subsequent operation. The subsequent erosion operation is used to retrieve the lost targets. Finally, a further dilation operation and minimum operation is performed to ensure the accuracy of the proposed algorithm. The further experimental results show that the proposed INTHT method has a strong correction capability. While ensuring high correction accuracy, it also ensures that almost all targets are not lost. In addition, for the proposed INTHT correction algorithm, due to the construction of two different, but related, structural operators and the appropriate morphological operation, we believe, to the best of our knowledge, that the algorithm not only has accurate stray light correction capability, but also greatly reduces its sensitivity to the size of the structural operator.

**Funding.** National Natural Science Foundation of China (61627819, 61727818, 6187030909); Technology Development Program of Jilin Province (20180201012GX); National Key Research and Development Program of China (2016YFF0103603).

**Disclosures.** The authors declare no conflicts of interest.

## REFERENCES

1. H. Wirnsberger, O. Baur, and G. Kirchner, "Space debris orbit predictions using bi-static laser observations. Case study: ENVISAT," Adv. Space Res. **55**, 2607–2615 (2015).
2. B. Esmiller, C. Jacquelard, H. Eckel, and E. Wnuk, "Space debris removal by ground-based lasers: main conclusions of the European project CLEANSPACE," Appl. Opt. **53**, I45–I54 (2014).
3. J. Nunez, A. Nunez, F. J. Montojo, and M. Condominas, "Improving space debris detection in GEO ring using image deconvolution," Adv. Space Res. **56**, 218 (2015).
4. X.-X. Zhang, B. Chen, F. He, K.-F. Song, L.-P. He, S.-J. Liu, Q.-F. Guo, J.-W. Li, X.-D. Wang, H.-J. Zhang, H.-F. Wang, Z.-W. Han, L. Sun, P.-J. Zhang, S. Dai, G.-X. Ding, L.-H. Chen, Z.-S. Wang, G.-W. Shi, X. Zhang, C. Yu, Z.-D. Yang, P. Zhang, and J.-S. Wang, "Wide-field auroral imager onboard the Fengyun satellite," Light Sci. Appl. **8**, 47 (2019).
5. J. Sharma, G. H. Stokes, C. von Braun, G. Zollinger, and A. J. Wiseman, "Toward operational space-based space surveillance," Lincoln Lab. J. **13**, 309–334 (2002).
6. E. M. Gaposchkin, C. von Braun, and J. Sharma, "Space-based space surveillance with the spaced-based visible," J. Guidance Control Dynamics **23**, 148–152 (2000).
7. Z. Fei, W. Sen, D. Chao, and C. Zhiyuan, "Stray light control lens for Xing Long 1-meter optical telescope," Opt. Precis. Eng. **18**, 513–520 (2010).
8. Y. Wang and E. J. Ientilucci, "A practical approach to Landsat 8 TIRS stray light correction using multi-sensor measurements," Remote Sens. **10**, 589 (2018).
9. X. Zhong, Z. Su, G. Zhang, Z. Chen, Y. Meng, D. Li, and Y. Liu, "Analysis and reduction of solar stray light in the nighttime imaging camera of Luojia-1 satellite," Sensors **19**, C2 (2019).
10. D. Liu, X. Wang, Y. Li, Z. Xu, J. Wang, and Z. Mao, "Space target detection in optical image sequences for wide-field surveillance," Int. J. Remote Sens. **41**, 1–12 (2020).
11. D. Liu, X. Wang, Y. Li, Z. Xu, J. Wang, and W. Liu, "Space target extraction and detection for wide-field surveillance," Astron. Comput. **32**, 100408 (2020).
12. T. Hardy, S. Cain, J. Jeon, and T. Blake, "Improving space domain awareness through unequal-cost multiple hypothesis testing in the space surveillance telescope," Appl. Opt. **54**, 5481–5494 (2015).
13. T. Hardy, S. Cain, and T. Blake, "Unequal a priori probability multiple hypothesis testing in space domain awareness with the space surveillance telescope," Appl. Opt. **55**, 4036–4046 (2016).
14. M. E. Feinholz, S. J. Flora, S. W. Brown, Y. Zong, K. R. Lykke, M. A. Yarbrough, B. C. Johnson, and D. K. Clark, "Stray light correction algorithm for multichannel hyperspectral spectrographs," Appl. Opt. **51**, 3631–3641 (2012).
15. A. Gerace and M. Montanaro, "Derivation and validation of the stray light correction algorithm for the thermal infrared sensor onboard Landsat 8," Remote Sens. Environ. **191**, 246–257 (2017).
16. M. Montanaro, A. Gerace, and S. Rohrbach, "Toward an operational stray light correction for the Landsat 8 thermal infrared sensor," Appl. Opt. **54**, 3963–3978 (2015).
17. S. Lu and C. L. Tan, "Binarization of badly illuminated document images through shading estimation and compensation," in *Ninth International Conference on Document Analysis and Recognition* (2007), Vol. **1**, pp. 312–316.
18. J. Wen, S. Li, and J. Sun, "A new binarization method for non-uniform illuminated document images," Pattern Recogn. **46**, 1670–1690 (2013).
19. N. Liu and J. Xie, "Interframe phase-correlated registration scene-based nonuniformity correction technology," Infrared Phys. Technol. **69**, 198–205 (2015).
20. X. Bai, S. Zhang, B. Du, Z. Liu, T. Jin, B. Xue, and F. Zhou, "Survey on dim small target detection in clutter background: wavelet, inter-frame and filter based algorithms," Procedia Eng. **15**, 479–483 (2011).
21. S. D. Deshpande, M. Hwa Er, R. Venkateswarlu, and P. Chan, "Max-mean and max-median filters for detection of small-targets," Proc. SPIE **3809**, 74–83 (1999).

22. X. Bai, F. Zhou, and Y. Xie, "New class of top-hat transformation to enhance infrared small targets," J. Electron. Imaging **17**, 030501 (2008).
23. J. Jie, L. Liu, and G. J. Zhang, "Robust and accurate star segmentation algorithm based on morphology," Opt. Eng. **55**, 151356 (2016).
24. T. Sun, F. Xing, J. Bao, S. Ji, and J. Li, "Suppression of stray light based on energy information mining," Appl. Opt. **57**, 9239–9245 (2018).
25. J. Xi, D. Wen, O. K. Ersoy, H. Yi, D. Yao, Z. Song, and S. Xi, "Space debris detection in optical image sequences," Appl. Opt. **55**, 7929–7940 (2016).
26. Z. Xu, C. Hu, C. Yan, and C. Gu, "Vane structure optimization method for stray light suppression in a space-based optical system with wide field of view," Opt. Eng. **58**, 191029 (2019).